

# Polarization dependence of x-ray absorption spectra in $\text{Na}_x\text{CoO}_2$

T. Kroll<sup>1,\*</sup>, A.A. Aligia<sup>2</sup>, and G.A. Sawatzky<sup>3</sup>

<sup>1</sup>*IFW Dresden, P.O. Box 270016, D-01171 Dresden, Germany*

<sup>2</sup>*Comisión Nacional de Energía Atómica, Centro Atómico Bariloche and Instituto Balseiro, 8400 S. C. de Bariloche, Argentina and*

<sup>3</sup>*Department of Physics and Astronomy, University of British Columbia, 6224 Agricultural Road, Vancouver, British Columbia, Canada V6T 1Z1*

In order to shed light on the electronic structure of  $\text{Na}_x\text{CoO}_2$ , and motivated by recent Co L-edge X-ray absorption spectra (XAS) experiments with polarized light, we calculate the electronic spectrum of a  $\text{CoO}_6$  cluster including all interactions between 3d orbitals. We obtain the ground state for two electronic occupations in the cluster that correspond nominally to all O in the  $\text{O}^{-2}$  oxidation state, and  $\text{Co}^{+3}$  or  $\text{Co}^{+4}$ . Then, all excited states obtained by promotion of a Co 2p electron to a 3d electron, and the corresponding matrix elements are calculated. A fit of the observed experimental spectra is good and points out a large Co-O covalency and cubic crystal field effects, that result in low spin Co 3d configurations. Our results indicate that the effective hopping between different Co atoms plays a major role in determining the symmetry of the ground state in the lattice. Remaining quantitative discrepancies with the XAS experiments are expected to come from composition effects of itineracy in the ground and excited states.

PACS numbers:

## I. INTRODUCTION

In recent years, there has been intense research on doped cobaltates because of their interesting transport, magnetic and superconducting properties.  $\text{Na}_x\text{CoO}_2$  shows an exceptionally high thermopower over the doping range  $0.5 \leq x \leq 0.9$ , while also displaying low resistivity and low thermal conductivity [1, 2]. These properties are those wished in materials with potential technological applications in refrigeration. In 2003 Takada and coworkers found a superconducting state in  $\text{Na}_{0.3}\text{CoO}_2 \cdot 1.3\text{H}_2\text{O}$  at temperatures lower than 5 K [3]. The system  $\text{Na}_x\text{CoO}_2$  is also interesting because of its similarities to the high- $T_c$  copper oxide superconductors, since both systems contain alternating layers consisting of oxygen and spin-1/2 transition metal ions separated by layers of lower conductivity in an anisotropic crystal structure.  $\text{Na}_x\text{CoO}_2$  consists of alternating layers of  $\text{CoO}_2$  and sodium, and becomes superconducting only when hydrated with water ( $\text{Na}_{0.35}\text{CoO}_2 \cdot 1.3\text{H}_2\text{O}$ ) [3]. However, in contrast to most cuprates, the  $\text{CoO}_2$  layers consist of edge-sharing  $\text{CoO}_6$  octahedra, arranged in such a way that the cobalt and oxygen ions form a triangular lattice. The superconducting resonance-valence-bond state for which some indications exist in the square lattice of the cuprates [4, 5], is believed to be favored in a triangular lattice [6].

In the most simple picture, the effect of sodium doping is only to modify the nominal ratio of  $\text{Co}^{3+}$  to  $\text{Co}^{4+}$  depending on the sodium content. This in turn, as in the cuprates, modifies the number of free carriers and affects dramatically the conducting and magnetic prop-

erties of the system.  $x = 0$  corresponds to the highly correlated (charge transfer or Mott) insulating limit. Magnetic susceptibility measurements [2, 7] have shown evidence of antiferromagnetic long-range order below 20 K in a doping range of  $0.75 \leq x \leq 0.9$ . From anisotropic dc magnetic susceptibility and  $\mu\text{SR}$  measurements on a  $\text{Na}_{0.82}\text{CoO}_2$  crystal one concludes that the Co spin is oriented along the crystal *c* axis [7].

Detailed knowledge of the electronic structure of this system is of course important for the understanding of all its properties. Ideally, from the knowledge of important parameters such as the  $d - d$  Coulomb interaction which includes exchange, the different hopping terms, and the charge-transfer energy one directly gains information about the band gap and the character of the electronic structure as it is explained in the classification scheme done by Zaanen, Sawatzky, and Allen [8]. Additionally, knowing important orbitals and interactions in an intermediate energy scale accessible in optical experiments, like the three-band Hubbard model in the case of cuprates [9], one would derive an effective low-energy model (like the  $t - J$  model based on Zhang-Rice singlets [10, 11, 12, 13, 14] for the cuprates) which describes the relevant low-energy physics. As an example, interesting phenomena have been explained by the formation of the Zhang-Rice singlets, such as the unusual magnetic and transport properties in  $(\text{La}, \text{Ca})_x\text{Sr}_{14-x}\text{Cu}_{24}\text{O}_{41}$  [15] and other cuprates. Similar low-energy reduction procedures have been followed for the nickelates [16] and magnetic double perovskites [17]. Instead, a systematic low-energy reduction has not been carried out for  $\text{Na}_x\text{CoO}_2$  and it seems that no consensus exists on the low-energy effective theory, in spite of the experimental and theoretical effort concerning the electronic structure of the system. At energy scales of 1 eV or larger, valuable information on this electronic structure is provided by local spectro-

\*Electronic address: [t.kroll@ifw-dresden.de](mailto:t.kroll@ifw-dresden.de)

scopic probes, like x-ray absorption spectroscopy (XAS) [18, 19], and x-ray photoemission (XPS) [20], while angle resolved photoemission (ARPES) [21, 22, 23] brings information on the dispersion relation just below the Fermi energy. In particular XAS, including a recent study of its dependence on the polarization of the incident light [18, 19], indicate that  $\text{Na}_x\text{CoO}_2$  exhibits the character of a doped charge-transfer insulator [8], rather than a doped Mott–Hubbard insulator, and the ground state contains a significant O 2p portion. Several calculations of the band structure use a single band effective model [6, 24, 25, 26, 27]. These descriptions can be justified if the lattice distortion or crystal field break the degeneracy of the 3d  $t_{2g}$  orbitals which are otherwise degenerate in a cubic environment, and if the O degrees of freedom can be integrated out in a similar way as in the cuprates. However, Koshiba and Maekawa based on an estimation of the effects of the above mentioned lattice distortion, and simple geometrical arguments, proposed an alternative scenario, with four interpenetrating Kagomé sublattices hidden in the  $\text{CoO}_2$  layer [28]. This scenario was further supported by Indergand *et al.* who derived the different hopping elements and interactions in the ensuing multi-band model [29]. Starting from this picture, Khaliulin *et al.* argued that the spin-orbit coupling of the correlated electrons on the  $t_{2g}$  level, although relatively small ( $\sim 80$  meV [31]) strongly influences the coherent part of the wave functions and the Fermi surface topology at low doping and favors triplet superconductivity, in marked contrast to the cuprates [30].

In this work, we solve exactly a cluster composed of a Co atom and its six nearest-neighbor O atoms for the geometry and oxidation states relevant to  $\text{Na}_x\text{CoO}_2$ . The aim is to learn more about the electronic structure of the system in an intermediate energy scale by comparison with experimental results on the polarization dependence of XAS spectra [19]. We confirm previous results concerning the highly covalent Co-O bond and the low spin state of Co [18, 19]. In addition an analysis of the dependence of the XAS intensities on the polarization direction of the incident light, support the scenario of Koshiba and Maekawa that the effective Co-Co hopping through the intermediate O sites is an essential part of the low energy physics. Additionally it will be shown, that due to the strong covalency a large amount of holes reside at the oxygen sites.

The formalism and relevant equations are presented in Section II. The results and its comparison to experiment are included in Section III. Section IV contains a summary and discussion.

## II. METHOD

### A. The model

An adequate starting point to describe the electronic structure of  $\text{Na}_x\text{CoO}_2$  is a multiband Hubbard model in-

cluding all Co 3d orbitals and O 2p orbitals, and their interactions (like the three-band Hubbard model for the cuprates [9]). This model cannot be solved exactly and one has to resort to some approximation. Calculations starting from first principles approximate the interactions and are known to lead to wrong results when the on-site Coulomb repulsion  $U_d$  between transition-metal 3d electrons is important. For example, they predict that  $\text{LaCuO}_4$  is a paramagnetic metal, while experimentally it is an antiferromagnetic insulator. In this work we take the opposite approach and retain exactly all 3d-3d interactions at the price to consider only one Co atom and its six nearest-neighbor O atoms, with octahedral  $O_h$  symmetry. The effects of the distortions are discussed in section III. We also make some additional approximations which are not essential but reduce the size of the matrices of the Hamiltonian in each symmetry sector. This allows us to have a calculational tool flexible enough to allow a fit of the XAS spectra in a reasonable amount of computer time. For example, we neglect the interactions between O 2p holes and this allows us to take advantage of a restricted basis for these orbitals which has the same symmetry as the 3d  $t_{2g}$  and  $e_g$  orbitals. The other O 2p orbitals become irrelevant in the absence of O-O interactions. For the description of the Co L-edge XAS spectra, we also need to include in the Hamiltonian the energy of the Co 2p core hole and its repulsion with the Co 3d holes [9, 32, 33].

The Hamiltonian that describes the dynamics of holes inside the  $\text{CoO}_6$  cluster is

$$\begin{aligned}
 H = & \sum_{\alpha \in t_{2g}, \sigma} \epsilon_{t_{2g}} d_{\alpha\sigma}^+ d_{\alpha\sigma} + \sum_{\alpha \in e_g, \sigma} \epsilon_{e_g} d_{\alpha\sigma}^+ d_{\alpha\sigma} + \sum_{jm} \epsilon_j c_{jm}^+ c_{jm} \\
 & + \sum_{i\alpha\sigma} \epsilon_{\text{O}} p_{i\alpha\sigma}^+ p_{i\alpha\sigma} + \sum_{i \neq j, \alpha\beta\sigma} t_i^{\alpha\beta} (p_{i\alpha\sigma}^+ d_{\beta\sigma} + \text{H.c.}) \\
 & + \sum_{i \neq k, \alpha\beta\sigma} \tau_{ij}^{\alpha\beta} p_{i\alpha\sigma}^+ p_{k\beta\sigma} + \frac{1}{2} \sum_{\lambda\mu\nu\rho} V_{\lambda\mu\nu\rho} d_{\lambda}^+ d_{\mu}^+ d_{\rho} d_{\nu} \\
 & + U_{cd} \sum_{j m \alpha \sigma} c_{jm}^+ c_{jm} d_{\alpha\sigma}^+ d_{\alpha\sigma}.
 \end{aligned} \tag{1}$$

Here  $p_{i\alpha\sigma}^+$  creates a hole on the O 2p orbital  $\alpha$  at site  $i$  with spin  $\sigma$ . The operator  $d_{\alpha\sigma}^+$  has an analogous meaning for the Co 3d orbitals. Similarly  $c_{jm}^+$  creates a Co 2p core hole with angular momentum  $j$  and projection  $m$ .

The first two terms of Eq. (1) describe the energy of the  $t_{2g}$  and  $e_g$  Co 3d orbitals split by a crystal field  $\epsilon_{t_{2g}} - \epsilon_{e_g} = 10Dq$ . We note that this difference can be called the “ionic” contribution to the crystal field splitting, since after hybridization with the O orbitals, the difference between mixed  $t_{2g}$  and  $e_g$  orbitals is much larger due to what is called the ligand field contributions. The third term describes the energy of the Co core hole, with a splitting  $\epsilon_{3/2} - \epsilon_{1/2} \sim 15$  eV. The fourth term corresponds to the energy of the O 2p orbitals. The next two terms represent the Co-O and O-O hopping, parametrized as usual, in terms of the Slater-Koster parameters [34]. The

term before the last includes all interactions between 3d orbitals originated by the Coulomb repulsion of electrons in the 3d shell. The last term describes the repulsion between the Co 3d holes and a Co 2p core hole if present. We have neglected the exchange and higher multipole Coulomb interactions between these orbitals. Their effects will be discussed later. Spin-orbit coupling of the 3d electrons is negligible compared with the other energies in the problem ( $\sim 80$  meV [31]) and was also neglected.

The matrix elements of the interactions inside the 3d shell are given by [35]

$$V_{\lambda\mu\nu\rho} = \int d\mathbf{r}_1 d\mathbf{r}_2 \bar{\varphi}_\lambda(\mathbf{r}_1) \varphi_\mu(\mathbf{r}_2) \frac{e^2}{|\mathbf{r}_1 - \mathbf{r}_2|} \varphi_\nu(\mathbf{r}_1) \varphi_\rho(\mathbf{r}_2), \quad (2)$$

where  $\varphi_\lambda(\mathbf{r}_1)$  is the wave function of the spin-orbital  $\lambda$ . We have calculated all these integrals in terms of the Slater parameters  $F_0$ ,  $F_2$ , and  $F_4$  using known methods of atomic physics [36, 37]. The resulting form of this interaction term is long and we do not reproduce it here. The terms including only  $t_{2g}$  orbitals are described in Ref [38], and those among  $e_g$  ones are described for example in Ref. [16]. Some of the remaining terms are listed in Ref. [37]. In particular, the value of the Coulomb repulsion between electrons of opposite spin at the same orbital is  $U_d = F_0 + 4F_2 + 36F_4$ , and the spin-spin interaction between 3d orbitals of the same irreducible representation is  $J_{t_{2g}} = 3F_2 + 20F_4$ , and  $J_{e_g} = 4F_2 + 15F_4$ .

In  $\text{Na}_x\text{CoO}_2$ , the formal oxidation state of the O ions is -2, and that of Co depends on the sodium content  $x$ , being  $\text{Co}^{3+}$  for  $x = 1$ , and  $\text{Co}^{4+}$  for  $x = 0$ . This means that our cluster has to be solved for a total of four holes (configurations  $d^6L^0$ ,  $d^7L^1$ ,  $d^8L^2$ , etc.) in the former case and five holes (configurations  $d^5L^0$ ,  $d^6L^1$ , etc.) in the latter. The respective probabilities are assumed to be  $x$  and  $1 - x$ . For simplicity, we will label these two cases as  $\text{Co}^{3+}$  and  $\text{Co}^{4+}$  respectively, although as we shall see there is a significant degree of covalency and the real Co oxidation states are smaller.

## B. The x-ray absorption intensity

The ground state of the cluster in both above mentioned cases (for  $\text{Co}^{3+}$  and  $\text{Co}^{4+}$ ) does not contain any Co 2p core hole. The excitation with light promotes a Co 2p electron to the Co 3d shell, or in other words, creates a core hole and destroys a 3d hole. In the dipolar approximation, the effect of the light is calculated in time-dependent perturbation theory from the addition of the term  $\mathcal{H}_L = \mathbf{p} \cdot \mathbf{A}$  to the Hamiltonian, where  $\mathbf{p}$  is the momentum operator and  $\mathbf{A} = (A_x, A_y, A_z)$  is the vector potential. Except for an unimportant prefactor, the relevant part of  $\mathcal{H}_L$  can be deduced from symmetry arguments and general physical considerations: it should be rotationally invariant, spin independent, and contain terms that destroy a 3d hole and create a core hole. This

leads to the operator

$$\mathcal{H}_L = \sum_{l_z\sigma} (O_{2l_z\sigma}^+ d_{2l_z\sigma} + \text{H.c.}) \quad (3)$$

Here the destruction operators of the 3d holes  $d_{2l_z\sigma}$  are expressed in terms of  $l_z$ , the orbital angular momentum projection.  $O_{2l_z\sigma}^+$  is an irreducible operator that transforms like an angular momentum  $L = 2$  with projection  $l_z$ , constructed combining the components of  $\mathbf{A}$  in spherical harmonics ( $A_{1l_z}$ ) with the core hole operators  $c_{1l_z\sigma}^+$  that create a Co 2p hole with angular momentum projection  $l_z$  and spin  $\sigma$ . The expression of the five components of  $O_{2l_z\sigma}^+$  ( $l_z = -2$  to 2) is derived easily using Clebsch-Gordan coefficients. Similarly, using these coefficients, it is easy although lengthy, to express the light operator  $\mathcal{H}_L$  in terms of the basis for the orbitals used in the Hamiltonian (Eq. (1)) and Cartesian coordinates of  $\mathbf{A}$ :

$$\mathcal{H}_L = \sum_{\beta j m \alpha \sigma} a_{\beta j m \alpha \sigma} A_\beta p_{jm}^+ d_{\alpha \sigma} + \text{H.c.} \quad (4)$$

This is the most convenient form for our purposes.

Using Fermi's golden rule and neglecting an unimportant prefactor, the XAS intensity becomes

$$I = \sum_i p_i |\langle f | \mathcal{H}_L | i \rangle|^2 \delta(E_f - E_i - \hbar\omega). \quad (5)$$

Here  $|i\rangle$ , is one of the two possible initial states (ground state for  $\text{Co}^{3+}$  or  $\text{Co}^{4+}$ ),  $p_i$  its probability that depends on the Na content, and  $E_i$  its energy. Similarly  $f$  labels the final states.  $\hbar\omega$  is the energy of the incoming light represented by the vector potential  $\mathbf{A}$ .

In order to simulate the measured spectra, we have broadened the delta functions appearing in Eq. (5) replacing them by a Lorentzian line shape with a full width of 0.5 eV at half maximum (FWHM) at the  $L_3$ -edge and 0.7 eV at the  $L_2$ -edge due to different life time broadening effects.

## III. RESULTS

### A. The structure of the ground state

There are already indications that the Co ions in  $\text{Na}_x\text{CoO}_2$  are in a low spin state [40, 41], supported also by the interpretation of XAS measurements using polarized light [18, 19]. This means that crystal field effects dominate over the exchange terms. In fact, from the parameters that best fit the experiment (see Table III), one sees that  $10Dq = 1.2$  eV. As mentioned in the previous section, this corresponds to the "ionic" part of the crystal field. The actual splitting is much larger due to the covalency effects which are also strong in the system. In table I we present an overview of the configurations present in

Co <sup>3+</sup> Groundstate	Co <sup>4+</sup> Groundstate
d <sup>6</sup>	0.30
d <sup>7</sup> L <sup>1</sup>	0.47
d <sup>8</sup> L <sup>2</sup>	0.20
d <sup>9</sup> L <sup>3</sup>	0.03
d <sup>10</sup> L <sup>4</sup>	0.00
	d <sup>5</sup> 0.14
	d <sup>6</sup> L <sup>1</sup> 0.40
	d <sup>7</sup> L <sup>2</sup> 0.35
	d <sup>8</sup> L <sup>3</sup> 0.10
	d <sup>9</sup> L <sup>4</sup> 0.01
	d <sup>10</sup> L <sup>5</sup> 0.00

TABLE I: Overview of the hole distribution for the ground states. The numbers give the hole distribution in percent.

the ground state for clusters with nominal oxidation state Co<sup>3+</sup> and Co<sup>4+</sup>.

The ground state for Co<sup>3+</sup> is a singlet with  $A_{1g}$  symmetry (for the sake of clarity we use capital letters to denote the irreducible representations of many-body states). For the cluster representing nominal Co<sup>3+</sup>, the most important configurations in the ground state are  $d^6$  (30%) and  $d^7L^1$  (47%), indicating a very strong covalency in the system. Note that the  $d^6$  population is smaller than the  $d^7L$  population and considerably less than 50% of the total. Such a behavior can only be explained if one takes more than one ligand hole into account. In a configuration containing only  $d^6$  and  $d^7L$  with a positive charge transfer gap  $\Delta_{CT} = E(d^{n+1}L) - E(d^n)$  (see table III), the  $d^6$  population will always be larger or equal to  $d^7L$ , but will never be smaller. Things change if one includes also configurations containing two ligand holes  $d^8L^2$  with sufficiently large hopping terms. In this case the relative hole population changes towards the  $d^7L$  configuration, so that even for a positive charge transfer gap  $\Delta_{CT}$  the dominant configuration can include a ligand hole. This is a rather important result since it demonstrates that the hybridization between all those states involving one or more ligand holes is large enough to produce a low energy state which in fact is lower than that of the starting  $d^6$  configuration containing no ligand holes. The  $d^6$  configuration corresponds to  $t_{2g}^6$  (all holes with  $e_g$  symmetry occupied). For simplicity, to reduce the size of the matrices in the fitting procedure, we neglect the configurations  $t_{2g}^5e_g^1$ . This is justified by the fact that the interaction term which mixes the 3d configurations  $t_{2g}^6$  and  $t_{2g}^5e_g^1$  is  $\lambda = \sqrt{3}(F_2 - 5F_4) \simeq 0.3$  eV (see Table III), is much smaller than the effective crystal-field splitting  $\sim 3$  eV. The amount of  $t_{2g}^5e_g^1$  3d configurations can be calculated by perturbation theory, but in any case, its influence on the XAS spectra is of the order of 1%. Similarly, for Co<sup>4+</sup>, we have neglected states with more than one 3d  $t_{2g}$  hole.

With these simplifications and because of the neglect of interactions between electrons at the O sites, the number of relevant states in the subspace in which the ground state for Co<sup>3+</sup> is, reduced to 7 singlets with  $A_{1g}$  symmetry. Similarly, the ground state for Co<sup>4+</sup> is obtained from six identical 38x38 matrices and corresponds to a

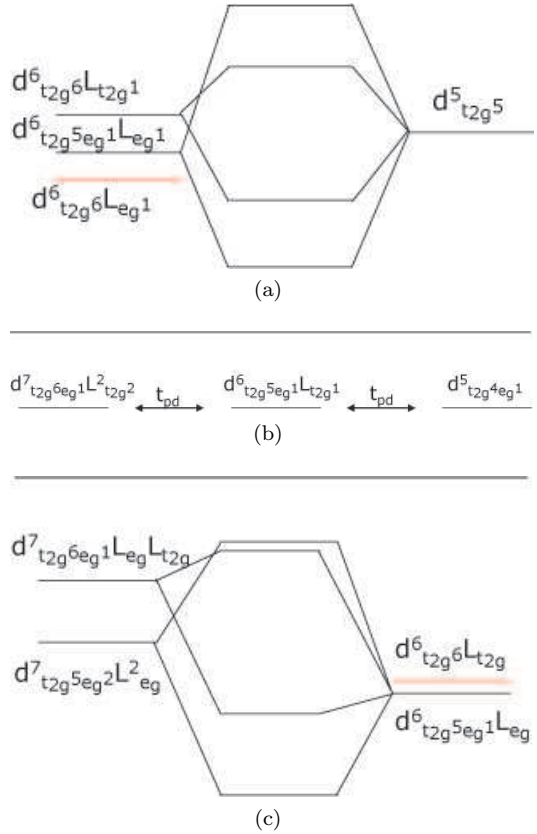


FIG. 1: Sketches of the energy scheme for different hole configurations of Co<sup>4+</sup>. (a): Hybridization between states with none and one ligand hole, (b) and (c): Hybridization between states with one and two ligand holes.

spin doublet with  $T_{2g}$  symmetry (this means three-fold orbital degeneracy).

Due to the symmetry of the cluster ( $O_h$ ), the 3d holes conserve its symmetry when they hop to the O 2p states. Neglecting the small amount of 3d  $t_{2g}^5e_g^1$  states in Co<sup>3+</sup>, the only possibility for a ligand hole is then a linear combination with  $e_g$  symmetry giving the configuration  $d_{t_{2g}6e_g1}^7L_{e_g1}$ .

Co <sup>4+</sup> (five holes)	
Ground state	
d <sup>5</sup>	0.14
d <sup>6</sup> L <sub>e<sub>g</sub></sub> <sup>1</sup>	0.37
d <sup>6</sup> L <sub>t<sub>2g</sub></sub> <sup>1</sup>	0.04
d <sup>7</sup> L <sub>e<sub>g</sub></sub> <sup>2</sup>	0.28
d <sup>7</sup> L <sub>e<sub>g</sub>1t<sub>2g</sub></sub> <sup>2</sup>	0.07

TABLE II: Hole distribution for the ground state of the Co<sup>4+</sup> cluster, including information of symmetry up to configurations with two ligand holes. The numbers give the hole distribution in percent.

A more complicated picture is expected for the cluster corresponding to Co<sup>4+</sup>, since it contains five holes meaning that there will always be one hole with  $t_{2g}$  symmetry

in the system (either at the Co site or distributed among the O ions). For the parameters that fit the experiment, the ground state of this cluster is a spin doublet with orbital symmetry  $T_{2g}$ . This three-fold degeneracy in the point group  $O_h$  is split by the rhombohedral distortion as discussed in the next subsection. While an overview of the structure of the ground state is given in table I, the distribution among different possible configurations up to two ligand holes for the ground state of the  $\text{Co}^{4+}$  octahedra is shown in table II. Note that states with one and two ligand holes dominate the composition of the ground state. The  $d^5$  configuration is very simple. It consists of four  $3d_{e_g}$  holes and one  $3d_{t_{2g}}$  hole, or equivalently it consists of five  $3d_{t_{2g}}$  electrons ( $d_{t_{2g}}^5$ ). The configurations with one ligand hole with the same symmetry are  $d_{t_{2g}}^5 e_g^1 L_{e_g^1}$ , and  $d_{t_{2g}}^6 L_{t_{2g}^1}$ . The former has a larger hybridization with the  $d^5$  configuration because the hopping between 3d and 2p  $e_g$  or  $t_{2g}$  electrons involves the Slater-Koster parameter ( $pd\sigma$ ) or ( $pd\pi$ ) respectively, and the former has a larger magnitude. For configurations with two ligand holes there are two configurations with  $T_{2g}$  symmetry:  $d_{t_{2g}}^6 L_{e_g^1} L_{t_{2g}^1}$  and  $d_{t_{2g}}^7 L_{e_g^2}$ . They both hybridize with the dominant one hole state  $d_{t_{2g}}^6 e_g^1 L_{e_g^1}$ . The only difference is that the first configuration couples via  $t_{2g}$  hopping to the one hole state while the second configuration couples via a  $t_{e_g}$  hopping which is larger and results in a stronger occupation of this state (see table II). Although it is allowed by symmetry, the above mentioned states with two ligand holes do not hybridize with the state  $d_{t_{2g}}^6 L_{t_{2g}}$  due to the particular structure of the wave functions.

From the above described distribution of holes in the  $\text{Co}^3$  and  $\text{Co}^4$  clusters, it turns out that the real Co valence for each cluster is 2.04 and 2.56 respectively, emphasizing again the very strong degree of covalency in these systems.

## B. Breaking of the octahedral symmetry

The edge-sharing  $\text{CoO}_6$  octahedra in a  $\text{CoO}_2$  layer of  $\text{Na}_x\text{CoO}_2$  are compressed along the  $c$  axis (oriented parallel to the (111) direction of one octahedra, see Fig. 2(a)). This distortion reduces the point group symmetry of our cluster to  $D_{3d}$ . As explained above, the ground state of the  $\text{Co}^{4+}$  cluster belongs to the  $T_{2g}$  representation of  $O_h$ . This representation is split in  $D_{3d}$  as  $T_{2g} = A'_{1g} + E'_g$ , where to avoid confusion, the representations of  $D_{3d}$  are primed. Labelling as  $|xy\rangle$ ,  $|yz\rangle$ , and  $|zx\rangle$  the basis functions of the representation  $T_{2g}$  (which in our case correspond to the many-body wave functions of the  $\text{Co}^{4+}$  cluster), the basis functions that transform irreducibly in  $D_{3d}$  can be written as

$$|A'_{1g}\rangle = \frac{1}{\sqrt{3}}(|xy\rangle + |yz\rangle + |zx\rangle) \quad (6)$$

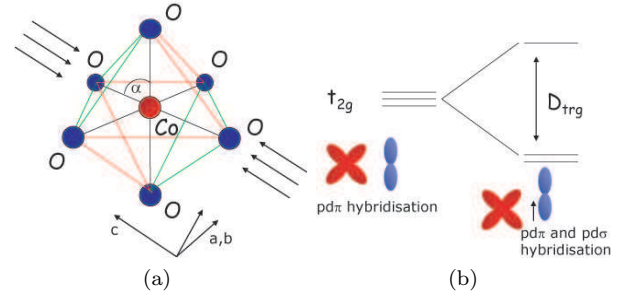


FIG. 2: (a): Distortion of the octahedra. (b): Splitting of the  $t_{2g}$  states in a trigonal crystal field.

for the state invariant under operations in  $D_{3d}$  and

$$|E'_g\pm\rangle = \frac{1}{\sqrt{3}}(|xy\rangle + e^{\pm i\frac{2\pi}{3}}|yz\rangle + e^{\pm i\frac{4\pi}{3}}|zx\rangle) \quad (7)$$

for the doubly degenerate states that transform like  $E'_g$ . A 3d orbital with the symmetry  $A'_{1g}$  looks like a  $3z^2 - r^2$  orbital and points into the direction of the crystallographic  $c$  axis. In a one-electron picture, for an adequate ordering of the energy of the orbitals, the  $\text{Co}^{4+}$  cluster would correspond to  $e'_g$  orbitals completely filled with 4 electrons and a half filled  $a'_{1g}$  orbital [7].

The rhombohedral distortion of the  $\text{CoO}_6$  octahedra is estimated by the deviation of the Co-O-Co bond angle from  $90^\circ$ . For example for  $x \approx 0.7$  Huang *et al.* find an angle  $\alpha \approx 96^\circ$  [46] which leads to a change of the thickness of one octahedra by 10%, assuming that the Co-O bond distance remains constant during the distortion.

From the fit of unpolarized XAS spectra [18], Wu *et al.* estimated  $D_{trg} = 1$  eV for the splitting  $D_{trg} = \langle E'_g \pm | \mathcal{H} | E'_g \pm \rangle - \langle A'_{1g} | \mathcal{H} | A'_{1g} \rangle$  between the many-body ground state  $A'_{1g}$  and the excited states  $|E'_g \pm\rangle$ . Instead, Koshibae and Maekawa using a point charge model obtained a negligible splitting and suggested that the band splitting at the zone center obtained in band structure calculations is dominated by the effective Co-Co hopping mediated by intermediate O atoms [28]. However, one expects that the splitting is dominated by covalency effects and that the ionic contribution plays a minor role. Very recently  $D_{trg} = 0.315$  eV has been obtained by an ab-initio quantum chemical configuration interaction method in a  $\text{CoO}_6$  cluster [44]. This is the most reliable result. The method used is known to provide accurate results for charge conserving excitations and has been used successfully in a large family of strongly correlated systems [44].

To check if the distortion affects our results for cubic symmetry, we have estimated the matrix element  $Q_{mix} = \langle E'_g \pm | \mathcal{H} | E'_g \pm, 2 \rangle$  between the  $E'_g$  states and the lowest excited states  $|E'_g \pm, 2\rangle$  of the same symmetry. These excited states belong to the irreducible representation  $E_g$  of  $O_h$  and therefore do not hybridize with the ground state in cubic symmetry. The only part of

the Hamiltonian where the trigonal distortion comes into play is a change in the hopping part through changes in relative orientations of the orbitals, and O-O distances. We assumed an  $r^{-3}$  distance dependence for the hopping between  $p$  orbitals [45]. We find  $Q_{mix} = -0.09$  eV. Since  $|Q_{mix}|$  is very small compared to the other energies of the model, in particular  $10Dq$  and the separation between  $T_{2g}$  and  $E_g$  levels, we can safely use the states obtained in cubic symmetry for the calculation of the XAS spectra.

A ground state with  $E'_g$  symmetry is incompatible with the XAS data. Therefore only a positive  $D_{trg}$  is consistent with experiment. The value  $D_{trg} = 0.315$  eV is smaller but of the order of magnitude of the band width reported in ab-initio calculations. A small value of  $D_{trg}$  would be consistent with the proposal of Koshibae and Maekawa [28] that the energy splitting does not originate in the crystal field, but is determined by the kinetic energy of the electrons. Within this picture, translated to our many-body states, and neglecting  $D_{trg}$ , the ground state for one  $\text{Co}^{4+}$  cluster moving in a lattice of  $\text{Co}^{3+}$  is a Bloch state with total wave vector  $K = 0$  in an effective Kagomé sublattice with point symmetry  $A'_{1g}$ . To keep it simple, restricting the wave function to only three sites, and one of the four Kagomé sublattices, the ground state would be

$$|g\rangle = \frac{1}{\sqrt{3}}(|1, xy\rangle + |2, yz\rangle + |3, zx\rangle), \quad (8)$$

where here  $|i, \alpha\rangle$  denotes a state composed of the ground state of one  $\text{Co}^{4+}$  cluster with symmetry  $\alpha$  at site  $i$ , and the (invariant  $A_{1g}$ ) ground state of the  $\text{Co}^{3+}$  cluster at the other two sites. However, the effective tight-binding Hamiltonian considering only the most important hopping term and neglecting  $D_{trg}$ , has a  $U(4)$  symmetry due to the equivalence between the four Kagomé sublattices, and the different possibilities of breaking of this symmetry leads to several scenarios for the ground state [29].

The difference between Eqs. (6) and (8) for the polarization dependence of the intensity in the XAS spectra, can be easily illustrated for the case in which the final states  $|f_\alpha\rangle$  in Eq. (5) for a  $\text{Co}^{4+}$  cluster have a core hole  $2p_\alpha$  ( $\alpha = x, y$ , or  $z$ ) with given spin, and the rest of the state (the holes of the 3d shell) belongs to the  $A_{1g}$  irreducible representation. This intensity with a factor two coming from spin, corresponds to the sum of the intensities of the peak A in Fig. 3 (for a total momentum  $j = 3/2$  of the core hole) and the corresponding peak at higher energies and lower intensity for  $j = 1/2$  (A' in Fig. 3). For incoming light in the direction  $\beta$ ,  $\mathcal{H}_L$  is proportional to the momentum operator in this direction  $\hat{p}_\beta$ . Then by symmetry, all matrix elements  $\langle f | \mathcal{H}_L | i \rangle$  entering Eq. (5) can be related to  $\gamma = \langle f_x | \hat{p}_y | xy \rangle$ . Using Eq. (6), it is easy to see that the contribution of these states (summed over  $\alpha$ ) to the intensity in the one-cluster picture, for  $\mathbf{A}$  is parallel and perpendicular to the  $c$  axis

becomes

$$I_{\parallel}^1 = 4|\gamma|^2/3, \quad I_{\perp}^1 = |\gamma|^2/3. \quad (9)$$

In the extended picture, naturally, the light operator is a sum over all sites of that already described. Taking again only three sites for simplicity, there are three possible final states for each core hole orbital  $2p_\alpha |i, f_\alpha\rangle$  depending on which site  $i$  was excited by the core hole. Adding these contribution one finds, using Eq. (5)

$$I_{\parallel}^{ext} = I_{\perp}^{ext} = 2|\gamma|^2/3. \quad (10)$$

Thus due to the loss of coherence, there is a factor 2 less intensity for  $\mathbf{A}$  parallel to  $c$  in the XAS spectra for the sum of the contributions of peaks A and A' (see Fig. 3) in the case in which the hole is distributed over one Kagomé sublattice. This factor is large enough to be detected by the experiment. In the latter case, the result is the same as for a ground state composed of statistical average of the three  $T_{2g}$  states and has no polarization dependence. The situation is different if the breaking of the above mentioned  $U(4)$  symmetry leads to some coherence between  $T_{2g}$  states at the same site. Note that the intensity is redistributed among the different directions but keeps the same angular average. This is due to the local character of the transition and the fact that only one irreducible representation involved in the initial state, final state and operator.

We shall show that our results point to an intermediate situation, but with dominance of the lattice effects over the on-site distortion.

### C. The XAS intensity

As mentioned above, the ground state for a  $\text{Co}^{3+}$  cluster is invariant under the symmetry operations of  $O_h$  and as a consequence, the corresponding XAS intensity is independent of the polarization of the incident light. Also, for  $\text{Co}^{4+}$ , the XAS intensity for a statistical average of the three states of the irreducible representation  $T_{2g}$  ( $|xy\rangle, |yz\rangle$  and  $|zx\rangle$ ) (which would correspond to a ground state like Eq. (8)) leads to the same intensity for  $\mathbf{A} \parallel c$  and  $\mathbf{A} \perp c$ .

Instead, using Eq. (6) for the ground state of  $\text{Co}^{4+}$ , one obtains a polarization dependence similar to the experiment, but more pronounced: The ratio of the intensities for excitations to a state with  $A_{1g}$  symmetry plus a core hole is  $I_{\parallel}^1/I_{\perp}^1 = 4$  (see Eq. (9)) whereas the experimental ratio has been found to be  $I_{\parallel}^{exp}/I_{\perp}^{exp} \approx 1.8$ . Therefore the experiment suggests an intermediate situation between the ground states (6) and (8). The actual many-body ground state of the system is out of the scope of our cluster calculations. In order to simulate this situation, we have calculated the spectrum

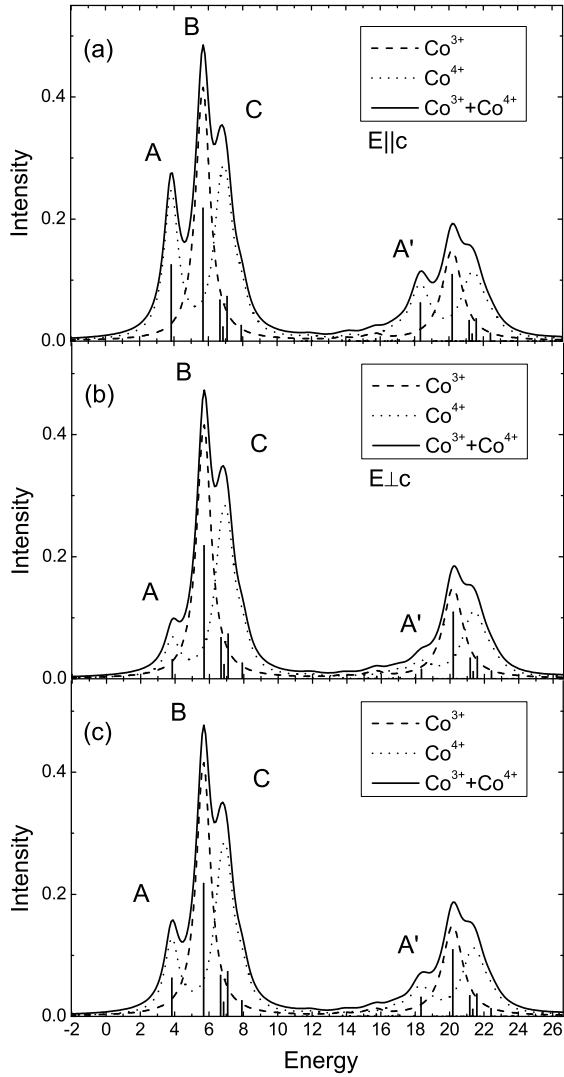


FIG. 3: XAS spectra for different polarizations: (a)  $E \parallel c$  and (b)  $E \perp c$ . Dashed line:  $\text{Co}^{3+}$  cluster. Dotted line:  $\text{Co}^{4+}$  cluster. Straight line: sum of both representing  $(\text{Na}_0.5\text{CoO}_2)$ . In (a) and (b) Eq. (6) was used for the ground state of the  $\text{Co}^{4+}$  cluster was used, while (c) corresponds to Eq. (6) giving a polarization independent result.

as a weighted average of Eqs. (9) and (10):

$$I_{\text{total}} = (1 - \xi)I_f^1 + \xi I_f^{\text{ext}} \quad (11)$$

with  $0 \leq \xi \leq 1$ . In order to get the observed experimental ratio for the  $A_{1g}$  peak  $\xi$  has to be approximately  $\xi = 0.73$ .

In Fig. 3 we show the results for the XAS intensity for the parameters indicated in Table III that best fit the experiment. As adjustable parameters, we have used  $F_0$  (or  $U_d = F_0 + 4F_2 + 36F_4$ ),  $\epsilon_0$  (or  $\Delta_{CT}(\text{Co}^{n+}) =$

$F_0 = 3.5$	$pd\sigma = 2.35$	$10Dq^i = 1.2$
$F_2 = 0.2$	$pd\pi = -1.0$	$\epsilon_p = 13$
$F_4 = 0.006$	$pp\sigma = 0.8$	$\Delta_{CT}(\text{Co}^{3+}) = 2.9$
$U_{dd} = 4.52$	$pp\pi = -0.2$	$\Delta_{CT}(\text{Co}^{4+}) = -1.1$

TABLE III: Best fit parameters, all parameters given in eV.

$E(d^{n+1}L) - E(d^n)$ ),  $10Dq$ ,  $(pd\sigma)$ , and  $(pp\sigma)$ . We have taken  $U_{dc} = U_d + 0.15$  eV.  $F_2$  and  $F_4$  were taken from values that fit approximately the energy separation between different terms in atomic spectra [39]. We assumed the relations  $(pd\pi) = -\sqrt{3}(pd\sigma)/4$ , and  $(pp\pi) = -0.81(pd\sigma)/3.24$  [45].

In terms of more fundamental parameters one has:

$$\begin{aligned} \Delta(\text{Co}^{3+}) &= \epsilon_0 - \epsilon_{e_g} - 3F_0 + 8F_2 - 33F_4 - pp\sigma + pp\pi \\ \Delta(\text{Co}^{4+}) &= \epsilon_0 - \epsilon_{e_g} - 4F_0 + 4F_2 - 37F_4/2 - pp\sigma + pp\pi, \end{aligned} \quad (12)$$

and correspond to the minimum energy necessary to promote a Co 3d hole to a linear combination of O 2p states in absence of Co-O hopping. If the O 2p hole is localized at one site,  $pp\sigma$  and  $pp\pi$  are absent in these equations and both  $\Delta(\text{Co}^{3+})$  increase in 1.0 eV.

To fit the experiments and explain the different observed structures, several configurations with considerable amount of ligand holes (described above) should be present in the ground state. This implies large covalency, and this in turn points to high hybridization, a low charge transfer gap  $\Delta_{CT}$  and low  $U_d$  in comparison with other transition metal oxides. Also, the relative position of the structures for  $\text{Co}^{3+}$  and  $\text{Co}^{4+}$  imply relatively large  $10Dq$  and low spin configurations. This is a rough explanation of the resulting parameters in Table III.

The  $\text{Co}^{3+}$  cluster (dashed line in Fig. 3) shows only one main peak at the  $L_{3,2}$  edge (peak (B) in the figure 3) which results from an excitation from the ground state with  $A_{1g}$  symmetry to an excited state with  $E_g$  symmetry and is polarization independent. Comparing to the similar system  $\text{LiCoO}_2$  which nominally contains only octahedra with four holes (i.e. a  $\text{Co}^{3+}$ -central ion) [47], one observes a weak structure on the high energy side of the  $e_g$  peak which is missing here because of the missing  $2p$ - $3d$  core hole exchange interaction. The  $\text{Co}^{4+}$  cluster shows two main structures at both edges. The lower energy peak structure (A) contains of a single peak and results from excitations into states with  $A_{1g}$  symmetry, while the higher energy peak structure (C) originates from many excitations of low intensity to final states with  $T_{1g}$  and  $T_{2g}$  symmetry. Only the former peak (A) shows a polarization dependence and is strong for incoming light polarized along the (111) direction (crystallographic  $c$  axis) and weak for polarization perpendicular to the (111) direction (in-plane polarization).

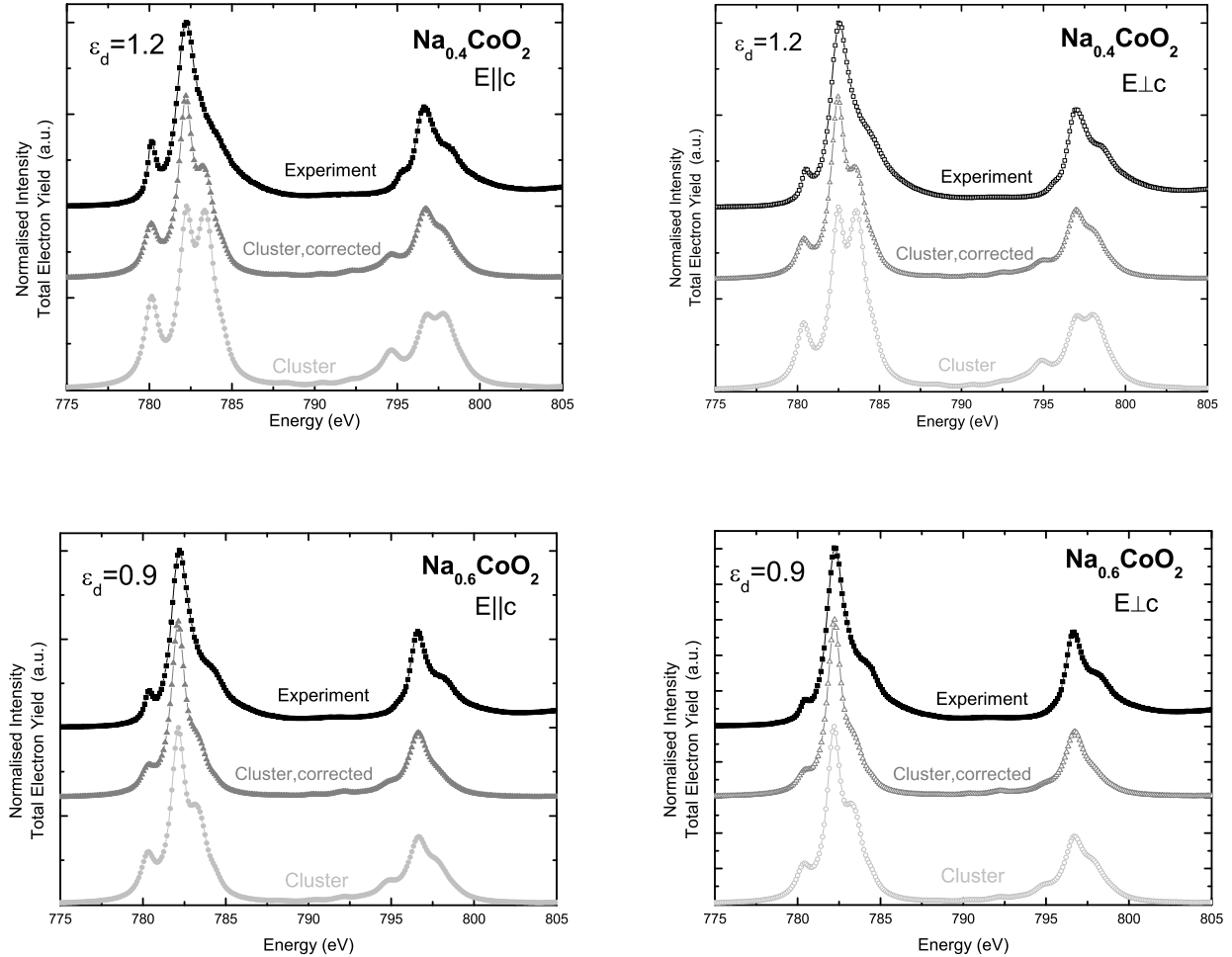


FIG. 4: Comparison of the theoretical results (bottom) with experimental data (top) for  $x=0.4$  and  $x=0.6$  for polarizations indicated inside each figure. In the middle curve the results are manipulated in such a way, that the intensity of the  $\text{Co}^{4+}$  cluster is decreased by a factor 2.0.

In Fig. 4 we compare the theoretical results with experimental data for the stoichiometries  $\text{Na}_{0.4}\text{CoO}_2$  and  $\text{Na}_{0.6}\text{CoO}_2$  as well as for polarization perpendicular and parallel to the crystallographic  $c$  axis. In the theoretical curve at the bottom, we have used the weighted average Eq. (11) with  $\xi = 0.73$  which best fits the polarization dependence of peaks A and A'. As explained above, this average redistributes the spectral weight among the different polarizations but does not affect the total intensity coming from a  $\text{Co}^{4+}$  cluster. As it is apparent comparing the bottom and top curves in Fig. 4, the above mentioned average is not enough to reach a quantitative agreement with experiment: there is still a disagreement in the intensity ratio between that coming from a  $\text{Co}^{4+}$  cluster and that originating from a  $\text{Co}^{3+}$  cluster. The theoretical contribution of  $\text{Co}^{4+}$  seems to be two times larger

than in the experiment for  $x=0.4$  (this ratio is a little bit less than two for  $x=0.6$ ). Wet chemical redox analysis point to a proportion of  $\text{Co}^{+4}$  smaller than that corresponding the nominal Na content [50]. This can explain part of the discrepancy. Another possible explanation for the discrepancy is the redistribution of spectral weight due to itineracy of the final states. The effects of the hopping in a model of two sites has been studied by G.A. Sawatzky and A. Lenselink [49]. In our case, these effects seem to be of minor importance for the peak A, because the expected magnitude of the hopping  $\sim 0.1$  eV [28] is much smaller than the energy difference between excited states involved ( $\sim 1.9$  eV). However they are certainly important for the higher energy multiplets.

Note that our neglect of the exchange interaction between the core hole and the 3d holes leads to slight change in the shape of the curves, but does not affect the total

intensities for both clusters.

Spin-orbit coupling inside the 3d shell, which we have neglected might also lead to a reduction of the intensity of the low energy peak at the  $L_2$ -edge that corresponds to peak A as an effect of selection rules [48]. However, in our case, the effect of spin-orbit coupling is small compared to the intersite hopping terms  $t \sim 0.1$  eV [28]. Therefore, our approach of considering a sixfold degenerate ground state for  $\text{Co}^4$  ( $T_{eg}$  doublet) instead of split doublet and quartet states is justified. Therefore, we expect that the reduction of intensity due to spin-orbit coupling inside the 3d shell is small.

The relative peak positions do not change upon doping, except for the  $A_{1g}$  peak. The distance between the main ( $E_g$ ) peak and the  $A_{1g}$  peak becomes smaller with increasing  $x$  (decreasing amount of  $\text{Co}^{4+}$  ions) [19]. This change is best simulated by a variation of the ionic crystal field  $10Dq$  from 1.2 eV ( $x=0.4$ ) to 0.9 eV ( $x=0.6$ ). A decreasing value of  $10Dq$  is also supported by Huang *et al.* who performed neutron diffraction on powder samples and found an increasing Co–O bond length with increasing doping [46]. This would change the total crystal field splitting (the ionic term  $10Dq$  plus the effects of hopping), but a slight change in the hopping parameters does not change the relative peak positions.

#### IV. SUMMARY AND DISCUSSION

We have investigated the local electronic structure around a Co atom in  $\text{Na}_x\text{CoO}_2$ , by solving exactly a  $\text{CoO}_6$  cluster (a basic octahedron of the system) containing the Co 3d and O 2p valence electrons, and with the appropriate charge according to the Na doping. We have included all interactions between 3d electrons in the cluster. For the calculation of the polarization dependence of the XAS spectrum, we have included the energy of the Co 2p core hole with its spin-orbit coupling  $\Delta_{SO} \sim 15$  eV, and its repulsion with the Co 3d holes. The exchange interaction between Co 2p and 3d holes has been neglected for simplicity. Due to comparatively large magnitude of  $\Delta_{SO}$ , crystal-field effects and covalency, one expect the influence of this term to be small in comparison to lighter 3d transition metals [42].

Within a purely local picture, assuming an  $A'_{1g}$  ground

state [Eq. (6)] and disregarding for the moment the total intensity of the  $\text{Co}^{4+}$  contribution, we are able to reproduce the essential features of the polarization dependent XAS experiments fairly well. Slight differences at the shoulders of the largest peaks originate from the neglect of the Co 2p-3d exchange interaction which would add an additional weak structure in this region, as shown by comparison with the case  $\text{LiCoO}_2$  [47].

Quantitatively, a fully coherent  $A'_{1g}$  ground state, as Eq. (6) leads to too large intensity ratio for peak A (and A') of the  $\text{Co}^{+4}$  contribution between light polarized parallel or perpendicular to the trigonal axis. This points out that a purely local picture is not fully consistent with experiment. In fact, the best fit corresponds to a  $\approx 70\%$  loss of coherence produced by delocalization. This redistribution of intensity among the different polarizations is consistent with an itinerant picture based on four Kagomé sublattices hidden in the  $\text{CoO}_2$  layer [28, 29] as a first approximation for the electronic structure.

The above mentioned redistribution is not enough to explain the large total amount of the  $\text{Co}^{+4}$  contribution to the intensity. Part of this discrepancy might be due to proportion of  $\text{Co}^{+4}$  smaller than that suggested by the nominal Na content [50]. A more quantitative calculation of the XAS spectrum requires to take into account the itineracy of holes in the ground state and the excited states after the creation of the core hole, which leads to spectral weight transfer between  $\text{Co}^{+4}$  and  $\text{Co}^{+3}$  contributions [49]. This is in principle possible if one combines the knowledge of the local transition matrix elements with an effective Hamiltonian for the motion of the holes through the lattice. This approach has been followed to calculate different optical properties of the cuprates.[9, 14, 51, 52, 53, 54] However, in this system this task is more difficult and is beyond the scope of the present paper.

#### Acknowledgments

This investigation was supported by the DFG project KL 1824/2, by the Deutscher Akademischer Austauschdienst (DAAD), by PICT 03-12742 of ANPCyT, Argentina and Canadian funding agencies NSERC, CFI, and CIAR. A.A.A. is partially supported by CONICET.

---

[1] I. Terasaki, I. Tsukada, and Y. Iguchi, Phys. Rev. B **65** 195106 (2002)

[2] M. Mikami, M. Yoshimura, Y. Mori, T. Sasaki, R. Fujinashi, and M. Shikano, Jpn. J. Appl. Phys. **42** 7383 (2003)

[3] K. Takada, H. Sakurai, E. Takayama-Muromachi, F. Izumi, R.A. Dilanian, and T. Sasaki, Nature **422** 53 (2003)

[4] P.W. Anderson, Science **235** 1196 (1987); G. Baskaran and P.W. Anderson, Phys. Rev. B **37** 580 (1988).

[5] C. D. Batista and A. A. Aligia, Physica C **264**, 319 (1996); C. D. Batista, L. O. Manuel, H. A. Ceccatto and A. A. Aligia, Europhys. Lett. **38**, 147 (1997).

[6] G. Baskaran, Phys. Rev. Lett. **91** 097003 (2003)

[7] S.P. Bayrakci, C. Bernhard, D.P. Chen, B. Keimer, R.K. Kremer, P. Lemmens, C.T. Lin, C. Niedermayer, and J. Strempfer, Phys. Rev. B **69** 100410(R) (2004).

[8] J. Zaanen, G.A. Sawatzky, and J.W. Allen, Phys. Rev. Lett. **55**, 418 (1985)

[9] M.S. Hybertsen, E.B. Stechel, W.M.C. Foulkes, and M.

Schlüter, Phys. Rev. B **45**, 10032 (1992); references therein.

[10] F.C. Zhang and T.M. Rice, Phys. Rev. B **37**, 3759 (1988)

[11] H. Eskes and G.A. Sawatzky, Phys. Rev. Lett. **61**, 1415 (1988)

[12] A. A. Aligia, M. E. Simon, and C.D. Batista, Phys. Rev. B **49**, 13061 (1994); references therein.

[13] L. F. Feiner, J. H. Jefferson, and R. Raimondi, Phys. Rev. B **53**, 8751 (1996); references therein.

[14] M. E. Simon, A. A. Aligia and E. R. Gagliano, Phys. Rev. B **56**, 5637 (1997); references therein.

[15] T. Kroll, R. Klingeler, J. Geck, B. Büchner, W. Selke, M. Hücker, A. Gukasov, Jour. of Magnetism and Magnetic Materials **290** 306 (2005)

[16] C. D. Batista, A. A. Aligia and J. Eroles, Europhys. Lett. **43**, 71 (1998); references therein.

[17] P. Petrone and A. A. Aligia, Phys. Rev. B **66**, 104418 (2002).

[18] W.B. Wu, D. J. Huang, J. Okamoto, A. Tanaka, H.J. Lin, F.C. Chou, A. Fujimori, and C.T. Chen, Phys. Rev. Lett. **94** 146402 (2005)

[19] T. Kroll, J. Geck, C. Hess, T. Schwieger, G. Krabbes, C. Sekar, D. Batchelor, M. Knupfer, H. Berger, J. Fink, and B. Büchner, cond-mat/0606518 (2006)

[20] A. Chainani, T. Yokoya, Y. Takata, K. Tamasaku, M. Taguchi, T. Shimojima, N. Kamakura, K. Horiba, S. Tsuda, S. Shin, D. Miwa, Y. Nishino, T. Ishikawa, M. Yabashi, K. Kobayashi, H. Namatame, M. Taniguchi, K. Takada, T. Sasaki, H. Sakurai, and E. Takayama-Muromachi, Phys. Rev. B **69** 180508(R) (2004)

[21] M. Z. Hasan, Y.D. Chuang, D. Qian, Y.W. Li, Y. Kong, A.P. Kuprin, A.V. Fedorov, R. Kimmerling, E. Rotenberg, K. Rossnagel, Z. Hussain, H. Koh, N.S. Rogado, M.L. Foo, and R.J. Cava, Phys. Rev. Lett. **92** 246402 (2004)

[22] H.B. Yang, S.C. Wang, A.K.P. Sekharan, H. Matsui, S. Souma, T. Sato, T. Takahashi, T. Takeuchi, J.C. Campuzano, R. Jin, B.C. Sales, D. Mandrus, Z. Wang, and H. Ding, Phys. Rev. Lett. **92** 246403 (2004)

[23] H.B. Yang, Z.H. Pan, A.K.P. Sekharan, T. Sato, S. Souma, T. Takahashi, R. Jin, B.C. Sales, D. Mandrus, A.V. Fedorov, Z. Wang, and H. Ding, Phys. Rev. Lett. **95** 146401 (2005).

[24] D.J. Singh, Phys. Rev. B **61** 13397 (2000).

[25] D.J. Singh, Phys. Rev. B **68** 020503(R) (2003)

[26] H. Rosner, S.L. Drechsler, G. Fuchs, A. Handstein, A. Wälte, K.-H. Müller, Braz. Jour. Phys. **33** 718 (2003).

[27] Q.H. Wang, D.H. Lee and P.A. Lee, Phys. Rev. B **69**, 092504 (2004).

[28] W. Koshibae and S. Maekawa, Phys. Rev. Lett. **91** 257003 (2003)

[29] M. Indergand, Y. Yamashita, H. Kusunose, and M. Sigrist, Phys. Rev. B **71**, 214414 (2004)

[30] G. Khaliullin, W. Koshibae, and S. Maekawa, Phys. Rev. Lett. **93** 176401 (2004).

[31] K.W. Blazey and K.A. Müller, J. Phys. C **16**, 5491 (1983).

[32] G. vanderLaan, C. Westra, C. Haas, and G.A. Sawatzky, Phys. Rev. B **23**, 4369 (1981).

[33] Y. Kakehashi and A. Kotani, Phys. Rev. B **29**, 4292 (1984).

[34] J.C. Slater and G.F. Koster, Phys. Rev. **94**, 1498 (1954); R.R. Sharma, Phys. Rev. B **19**, 2813 (1979).

[35] J.W. Negele and H. Orland, *Quantum Many-Particle Systems*, (Addison-Wesley, New York, 1988).

[36] E. U. Condon and G. H. Shortley, *Theory of Atomic Spectra*, (Cambridge University Press, Cambridge and New York, 1935).

[37] C. J. Ballhausen, *Ligand Field Theory*, (Mc Graw-Hill Book Company, New York, 1962).

[38] A. A. Aligia and M. A. Gusmão, Phys. Rev. B **70**, 054403 (2004).

[39] *Atomic Energy Levels*, edited by C.E. Moore (MBS, Washington D.C., 1958).

[40] T. Motohashi, R. Ueda, E. Naujalis, T. Tojo, I. Terasaki, T. Atake, M. Karppinen, and H. Yamauchi, Phys. Rev. B **67** 064406 (2003)

[41] G. Lang, J. Bobroff, H. Alloul, P. Mendels, N. Blanchard, and G. Collin, Phys. Rev. B **72** 094404 (2005)

[42] J. Zaanen, G.A. Sawatzky, J. Fink, W. Speier, and J.C. Fuggle, Phys. Rev. B **32** 4905 (1985)

[43] F. de Groot, Coordination Chemistry Reviews, to be published (2004)

[44] S. Landron and M.-B. Lepetit, cond-mat/0605454.

[45] W.A. Harrison, *Electron Structure and the Properties of Solids* (Freeman, San Francisco, 1980).

[46] Q. Huang, M.L. Foo, R.A. Pascal, Jr., J.W. Lynn, B.H. Toby, Tao He, H.W. Zandbergen, and R. J. Cava, Phys. Rev. B **70** 184110 (2004)

[47] J. van Elp, J.L. Wieland, H. Eskes, P. Kuiper, G.A. Sawatzky, F.M.F. de Groot, and T.S. Turner, Phys. Rev. B **44** 6090 (1991)

[48] W. Gawelda, M. Johnson, F.M.F. de Groot, R. Abela, C. Bressler, and M. Chergui, Jour. Am. Chem. Soc. (in press)

[49] G.A. Sawatzky and A. Lenselink J. of Chem. Physica **72**, 3748-3753 (1980).

[50] M. Karppinen, I. Asako, T. Motohashi, and H. Yamauchi, Phys. Rev. B **71**, 92105 (2005).

[51] L.F. Feiner, Phys. Rev. B **48**, 16857 (1993).

[52] M. E. Simon, A. A. Aligia, C. D. Batista, E.R. Gagliano and F. Lema, Phys. Rev. B **54**, R3780 (1996).

[53] F. Lema and A. A. Aligia, Phys. Rev. B **55**, 14092 (1997).

[54] J. Eroles, C.D. Batista and A.A. Aligia, Phys. Rev. B **59**, 14092 (1999).